submitted for publication in *Physical Review Letters* JLAB-ACC-00-02

DISPERSIVELY ENHANCED BUNCHING IN HIGH-GAIN FREE-ELECTRON LASERS

H.P. Freund
Science Applications International Corp., McLean, VA 22102

G.R. Neil
Thomas Jefferson National Accelerator Facility
12000 Jefferson Avenue, Newport News, VA 23606

A free-electron laser using a multi-segment optical klystron (MSOK) is studied using a 3-D simulation code for use as 4th generation light sources. The MSOK consists of multiple wiggler segments with dipole triplets in the gaps. The dipole triplets impose a dogleg trajectory that ballistically enhances the electron beam bunching and the gain in the following wiggler segment. There are three principal advantages of the MSOK over single-segment wiggler designs. First, the saturation length is drastically reduced. Second, the MSOK is significantly less sensitive to beam energy spread. Third, the linewidth is narrower and can be tuned by varying the dipole field strength. As a result, the MSOK is an ideal configuration for 4th generation light sources.

PACS Numbers: 41.60.Cr, 52.75.Ms

The free-electron laser (FEL) is the prime concept for future 4th generation light sources of high-brightness coherent x-rays [1-5]. These FELs are intended to operate in the Self Amplified Spontaneous Emission (SASE) mode where the spontaneous emission from an electron beam propagating through periodic wiggler magnets is amplified to high levels in a single pass. The need for SASE is due to the absence of (1) effective x-ray mirrors which prevents the possibility of oscillators, and (2) high power coherent x-ray sources which prevents the construction of amplifiers. While progress on x-ray lasers offers hope for future FEL amplifiers, the SASE FEL is presently the principal design concept. However, in view of technological constraints, the gain length for the SASE FEL is long and the total wiggler length required for saturation exceeds 100 meters.

In this paper, we describe a multi-stage optical klystron (MSOK) employing a multi-segment wiggler in which dispersive magnetic elements are located in the gaps between the wigglers. The optical klystron achieves high gain by using one wiggler segment to initiate the bunching process after which the electrons continue bunching ballistically. Bunching occurs either over a free space drift or by utilizing a magnetic dispersion section to produce an equivalent drift over a shorter *axial* length. Here, we employ dispersive elements that are composed of dipole triplets where the outermost dipoles have the same magnitudes (B_0) and lengths (L_d) and the center dipole has the same magnitude as the outermost dipoles but twice the length. This configuration is often referred to as a "-++-" configuration. Alternative configurations of magnetic transport are also possible. The effect of this dipole triplet is to impose a dogleg on the trajectory, thereby enhancing the ballistic bunching of the beam over that from the preceding wiggler segment. A unit cell of the structure is illustrated schematically in Fig. 1, and the overall structure is composed of many such unit cells.

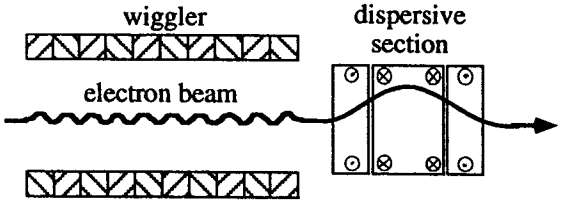

Fig. 1 Schematic illustration of a unit cell.

The optical klystron was first proposed for low-gain oscillators using two wiggler segments separated by a drift space by Vinokurov and Skrinsky [6], and has been implemented experimentally [7-11]. Low gain multi-component oscillators using a buncher, dispersive section and tapered wiggler have also been demonstrated [12]. A good theoretical discussion of optical klystrons for these low-gain oscillators is given by Elleaume [13]. The difference between low-gain oscillators and a SASE FEL is that in the latter the total gain is high and very long wigglers are required. Hence, optimization schemes for low-gain oscillators are not directly applicable to a high-gain MSOK.

Optical klystrons in high-gain FELs operating on the fundamental [14-16] and a harmonic [17] have also been discussed using two wigglers with a dispersive element in the gap. While it is not practicable for x-ray wavelengths, a low-gain oscillator using an optical klystron has been studied as a prebuncher for a beam that is then extracted from the optical cavity and injected into another wiggler for amplification to high powers [16]. In the high-gain harmonic generation experiment at Brookhaven National Laboratory [17], the first wiggler was tuned to a fundamental resonance at 10.6 microns, while the second wiggler was tuned to a fundamental at 5.3 microns. Injection of a high power seed pulse at 10.6 microns initiated bunching in the first wiggler. The dispersive dipoles enhanced the bunching prior to the second wiggler, resulting in enhanced gain in the second wiggler at 5.3 microns. The MSOK described here differs from past work in that (1) we are interested in x-ray wavelengths, (2) no harmonic interactions are involved, and (3) many such wiggler/dispersive sections are employed. It is shown that the overall system length, as well as the cumulative length of the wiggler, can be greatly reduced relative to a single-wiggler-segment SASE FEL using the MSOK.

Parameter	Value
Electron Beam	
Energy, E_b	14.35 GeV
Current, I_b	3400 A
Normalized Emittance, ε_n	1.5π mm-mrad
Energy Spread, $\Delta E_b/E_b$	0.02%
Wiggler	
Magnitude, B_w	13.2 kG
Period, λ_w	3.0 cm
Segment Length, L_w	4.8 m
Gap, L_g	2.0 m
Dispersive Segment	
Pole Length, L_d	0.4 m

Table 1 Electron beam, wiggler, and dipole parameters.

The 3D nonlinear, polychromatic simulation code MEDUSA [19-21] is used to simulate the interaction in the MSOK. MEDUSA employs planar wiggler geometry and treats the electromagnetic field as a superposition of Gauss-Hermite modes using a source-dependent expansion [20,22]. The field equations are integrated simultaneously with the 3D Lorentz force equations for an ensemble of electrons. No wiggler average is imposed on the orbit equations, and MEDUSA is capable of propagating the electron beam through both quadrupole and dispersive dipole magnetic sections. For simplicity, we assume that parabolic-pole face wigglers are used which eliminates he need for quadrupole focusing in the gaps between the wigglers. The interested reader is referred to the references for a detailed description of the code.

The example we consider is the Linac Coherent Light Source (LCLS) proposed by the Stanford Linear Accelerator Center as a 4th generation light source [1,3]. The electron beam parameters are shown in Table 1. The LCLS uses a single-segment wiggler with a 13.2 kG amplitude and a 3.0 cm period. We employ these values for the amplitude and period of each wiggler segment that is assumed to have a length of 4.8 m separated by 2.0 m gaps. These parameters yield a resonance at wavelengths near 1.49 Å. The dipoles are assumed to have 0.4 m lengths (for an overall length of 1.6 m for each triplet) and to be centered in the gaps. The number of unit cells in the MSOK and the dipole magnitude are varied in simulation to obtain the optimal performance. For this study, we consider uniform dipole and wiggler parameters; however, further performance enhancements may be possible by varying the wigglers and dipoles in stepwise fashion from unit cell to unit cell.

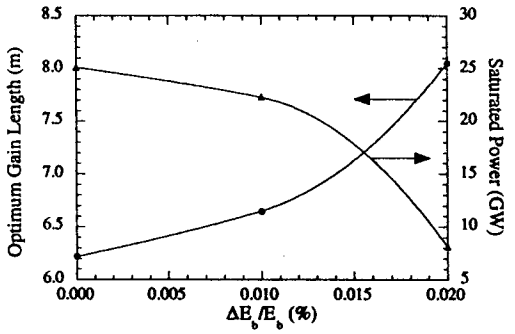

Fig. 2 Optimal gain length and saturated power versus energy spread for a long single-segment wiggler.

Before proceeding with the MSOK, we first characterize the single-segment performance [21]. A plot of the optimal gain length and saturated power versus energy spread for the single-segment wiggler is shown in Fig. 2. Note that the distance to saturation varies with the energy spread and the saturated power values occur for different wiggler lengths. Observe that the optimal gain length decreases relatively slowly from 6.21 m at $\Delta E_b/E_b$ = 0% to 6.64 m at $\Delta E_b/E_b$ = 0.01%, but increases rapidly thereafter and rises to 8.04 m when $\Delta E_b/E_b$

= 0.02%. The saturated power shows a similar sensitivity to energy spread. The essential conclusion is that performance for the single-segment wiggler configuration is extremely sensitive to the energy spread, and if the energy spread exceeds 0.02%, then the LCLS performance will suffer greatly. One of the advantages of the MSOK is a reduced sensitivity to energy spread.

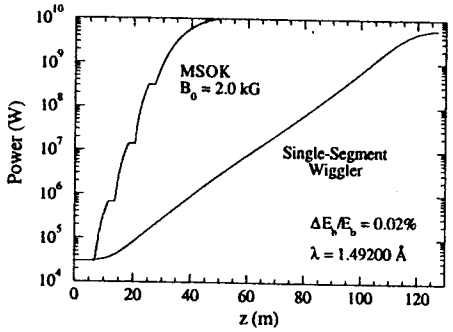

Fig. 3 Evolution of the power for the MSOK and a single-segment wiggler.

Now consider the performance of the MSOK with an energy spread of 0.02%. The optimal gain length is found at a wavelength of 1.4920 Å and we compare the evolution of a 30 kW seed pulse at this wavelength for both the single-segment wiggler and for the MSOK configuration. The optimal performance of the MSOK when $\Delta E_b/E_b = 0.02\%$ is found for $B_0 \approx 2.0$ kG and five wiggler segments. This consists of four unit cells followed by one longer wiggler segment that takes the interaction to saturation. The final wiggler segment is used to achieve saturation because the enhanced bunching due to the dispersive sections is less effective as the interaction nears saturation.

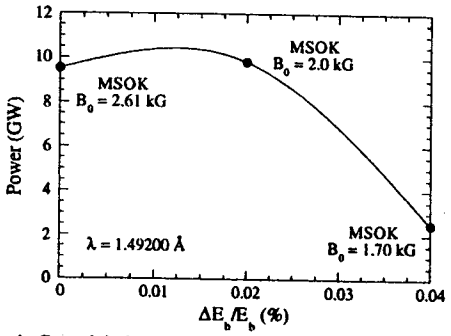

Fig. 4 Sensitivity of the MSOK to energy spread.

The evolution of the power with axial distance for the MSOK and the single-segment wiggler at a wavelength of 1.49200 Å is shown in Fig. 3. The single-segment wiggler saturates at a power of 5.63 GW over a distance of 127 m, while the MSOK saturates at a power of 9.84 GW over after at total length of 50 m with an aggregate wiggler length of 42 m. It is evident, therefore, that the MSOK is capable of achieving higher powers over a significantly shorter interaction length than the single-segment wiggler geometry. It should also be noted that the performance for the MSOK is virtually identical for energy spreads of 0.00% and 0.02% so that, at least for moderate values, the energy spread exacts no penalty for the MSOK.

The sensitivity of the MSOK to beam energy spread is important. Bearing in mind that the dipole magnitudes must be optimized for each choice of energy spread, we plot the output power versus energy spread for the MSOK in Fig. 4 for a total system length of 50 m (4 unit cells and a final longer wiggler segment) and for a wavelength of 1.4920 Å. It is evident, that the upper limit on the energy spread that the MSOK can tolerate without degradation of the power is about 0.02% for these parameters, which is twice that found for the single-segment wiggler. Further, the dipole magnitudes have been optimized to yield saturation over a distance of 50 m; hence, no lengthening of the interaction region is required to achieve saturation.

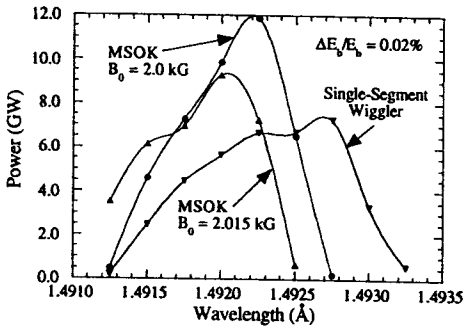

Fig. 5 Saturated power spectra for the MSOK and single-segment wiggler.

The bandwidth of microwave klystrons is very narrow, and it is expected that the MSOK will narrow the bandwidth of the FEL. This is indeed the case as shown in Fig. 5 where the power is plotted versus wavelength for the MSOK after a length of 50 m (with $B_0 = 2.00$ kG and $B_0 = 2.015$ kG) and with the single-segment wiggler after a distance of 127 m. These distances correspond to saturation at a wavelength of 1.4920 Å. It is evident from the figure that the spectral width (FWHM) has narrowed in the MSOK in comparison with the single-segment wiggler. In addition, it is possible to tune the peak in the spectral line of the MSOK over

the FEL gain band by varying the amplitudes of the dispersive dipoles, although a variation in the output power will accompany this retuning. However, the peak powers in the MSOK substantially exceed that found in the single-segment wiggler at the stated energy spread.

In summary, a detailed analysis has been presented of multi-stage optical klystron configuration for an application in an x-ray FEL using the three-dimensional FEL simulation code MEDUSA. This concept is relevant to designs for 4th generation light sources, and has the following advantages over the present conceptual designs:

1. The MSOK saturates in a significantly shorter distance than single-segment wiggler designs due to the enhanced bunching in the dispersive segments. Note that at least one recent SASE FEL experiment [4,5] employs multi-segment wigglers; however, this is for beam control (*i.e.*, focusing and steering) rather than for dispersive bunching and is formally equivalent to the single-segment wiggler.
2. The MSOK shows greatly reduced sensitivity to energy spread than a single-segment wiggler. For LCLS parameters, the MSOK has no penalty for energy spreads of about 0.02%. The MSOK achieves greater powers over shorter lengths (both overall and over the aggregate wiggler) than a single-segment design.
3. The FWHM linewidth of the MSOK is substantially narrower than the single-segment configuration and can be tuned over the FEL gain band by variations in the dipole field strengths. As a result, the FEL can be tuned "on-the-fly" without changes in the wiggler or beam parameters. Further, we speculate (without proof at this time) that this narrowing of the linewidth coupled with the enhanced dispersive bunching may reduce the sensitivity of the MSOK to shot noise.

The MSOK, therefore, is an ideal candidate for future 4th generation light sources.

Nevertheless, this paper is a preliminary study of the MSOK concept since we have used fixed length wigglers, gaps, and dipoles as well as uniform, repeated unit cells. It is expected that the performance can be further optimized by step tapers in some or all of these parameters. In addition, our analysis considered monochromatic wave growth. MEDUSA, however, can simulate the full polychromatic nature of the SASE FEL, and future work will extend the present analysis to this regime.

Computational work was supported the by Advanced Technology Group at SAIC under IR&D subproject 01-0060-73-0890-000. One of us (GRN) was supported by DOE Contract DE-AC05-84ER40150, and the Commonwealth of Virginia.

REFERENCES

1. M. Cornacchia et al., Free-Electron Laser Challenges, eds. P.G. O'Shea and H. Bennet, Proc. SPIE **2988**, 5 (1997).
2. B. Faatz et al., Nucl. Instrum. Meth. **A375**, 441 (1996).
3. see NTIS Doc. No. DE98059292 (LCLS Design Group, "LCLS Design Report," April 1998). Copies may be ordered from the National Technical Information Service, Springfield, VA 22162.
4. S.V. Milton et al., Free Electron Laser Challenges II, eds. H. Bennet and D. Dowell, Proc. SPIE **3614**, 86 (1999).
5. S.V. Milton et al., Phys. Rev. Lett. (submitted for publication).
6. N.A. Vinokurov and A.N. Skrinsky, Preprint INP 77-59, Novosibirsk (1977)
7. A.S. Artamonov et al., Nucl. Instrum. Meth. **177**, 247 (1980).
8. M. Billardon et al., J. de Physique-Colloque **44**, C1-29 (1983).
9. K. Yoshikawa et al., Nucl. Instrum. Meth. **A331**, 416 (1993).
10. K.W. Berryman and T.I. Smith, Nucl. Instrum. Meth. **A375**, 539 (1996).
11. V.N. Litvinenko, et al., Nucl. Instrum. Meth. **A429**, 151 (1999).
12. G.R. Neil et al., Nucl. Instrum. Meth. **A237**, 199 (1985).
13. P. Elleaume, J. de Physique-Colloque **44**, C1-333 (1983).
14. J.C. Gallardo and C. Pellegrini, Nucl. Instrum. Meth. **A296**, 448 (1990).
15. C.M. Tang and W.P. Marable, Nucl. Instrum. Meth. **A318**, 675 (1992).
16. J. Chen et al., Nucl. Instrum. Meth. **A375**, 299 (1996).
17. L.H. Yu et al. Nucl. Instrum. Meth. (to appear in 2000).
18. S.J. Hahn et al., Nucl. Instrum. Meth. **A358**, 167 (1995).
19. H.P. Freund and T.M. Antonsen, Jr., *Principles of Free-electron Lasers* (Chapman & Hall, London, 1996), 2nd edition.
20. H.P. Freund, S.G. Biedron, and S.V. Milton, IEEE J. Quantum Electron. (to appear in 2000).
21. H.P. Freund and P.G. O'Shea, Phys. Rev. Lett. (to appear in 2000).
22. P. Sprangle et al., Phys. Rev. Lett. **59**, 202 (1987); Phys. Rev. A **36**, 2773 (1987).